Supporting Information

Ultrastable Hydrido Gold Nanoclusters with the Protection of Phosphines

Shang-Fu Yuan,[1] Jiao-Jiao Li, [1] Zong-Jie Guan,[1,2] Zhen Lei[1] and Quan-Ming Wang [1,2,*]

[1]Department of Chemistry, Key Laboratory of Organic Optoelectronics and Molecular Engineering of the Ministry of Education, Tsinghua University, Beijing, 100084, P. R. China.

[2]Department of Chemistry, College of Chemistry and Chemical Engineering, Xiamen University, Xiamen, 361005, P. R. China.

Contents

I. Physical measurements

UV-Vis absorption spectra were recorded on a Shimadzu UV-2550 Spectrophotometer. Mass spectra were recorded on an Agilent Technologies ESI-TOF-MS. NMR data were recorded on a Bruker Advance II spectrometer (500MHz) (reference to external 85% H_3PO_4). ^{31}P NMR spectra was recorded in CD_2Cl_2, and referenced to external 85% H_3PO_4. ^{1}H NMR spectra were recorded in $CDCl_3$, chemical shifts (δ) were reported in parts per million (ppm) relative to TMS. ^{2}H NMR spectra were recorded in $CHCl_3$, residual solvent protons were used as a reference (δ, ppm, $CDCl_3$, 7.26).H_2 gas was analyzed on GC7920 Gas Chromatography equipped with TCD detector (N_2 carrier) at RT.

X-ray Crystallography. Intensity data of $\mathbf{1_H}$ and $\mathbf{2_H}$ were collected on an Agilent SuperNova Dual system (Cu Kα) at 100K and 173K, respectively. Absorption corrections were applied by using the program CrysAlis (multi-scan). The structures were solved by direct methods, and non-hydrogen atoms except SbF_6^- or PF_6^- counteranions, solvent and water molecules were refined anisotropically by least-squares on F_2 using the SHELXTL program. The hydrogen atoms of organic ligands were generated geometrically; $\mathbf{1_H}$ has large solvent accessible voids since a large number of disordered solvent molecules could not be resolved. A PF_6^- in $\mathbf{2_H}$ could not be located, but the formula reported was confirmed by mass spectrometry. SQUEEZE routine in PLATON was employed in the structural refinements of $\mathbf{2_H}$.

II. Synthesis

Materials and reagents.

Triphenyphosphine (Ph_3P, 99.5%), 2, 2'-bipyridylamine, Sodium borodeuteride ($NaBD_4$, 98.0%), Thiosalicylic acid (2-COOH-PhSH, 98%) and Silver hexafluoroantimonate ($AgSbF_6$, 98.0%) were purchased from J&K; sodium borohydride ($NaBH_4$, 98%) and other reagents employed were purchased from Sinopharm Chemical ReagentCo. Ltd. (Shanghai, China). Other reagents employed were commercially available and used as received.

$[Au_{20}(PPh_3)_{12}H_3](SbF_6)_3$ (1_H)

To a solution of Ph_3PAuCl (49 mg, 0.10 mmol) in CH_2Cl_2 (3.0 mL), $AgSbF_6$ (34 mg, 0.10 mmol) in methanol (2.0 mL) was added with vigorous stirring. After 60 min stirring at room temperature, the resulting solution was centrifuged for 3 min at 10000 r. min^{-1}, and the AgCl precipitate was filtered off. To this solution 2, 2'-bipyridylamine (34 mg, 0.2 mmol) was added, and EtONa (11 mg, 0.2 mmol) was subsequently added. After 30 min stirring at room temperature, a freshly prepared solution of $NaBH_4$ (1.8 mg in 1.0 mL of ethanol) was added dropwise with vigorous stirring. Thus, the ratio of $Ph_3PAuCl/NaBH_4$ is about 2:1. The solution color changed from orange to reddish-brown. After another 30 min stirring at room temperature, the mixture was refluxed at 50 ℃ in oil bath overnight, and finally to dark brown. Then the reaction was evaporated to dryness to give a dark brown solid. The solid was washed with ether (2×5.0 mL), then dissolved in 3.0 mL CH_2Cl_2:MeOH (v : v = 10 : 1), and the resulted solution was centrifuged for 3 min at 10000 r.min^{-1}. The brown supernatant was collected and subjected to vapor diffusion with ether : n-hexane (v : v = 1 : 5) to afford brown sheet-like crystals after 7 days in 5% yield. Red crystals of $[Au_8(Ph_3P)_8]^{2+}$ (6% yield) and black rods of $[Au_9(Ph_3P)_8]^{3+}$ (2% yield) were concomitantly crystallized, which could be separated from $\mathbf{1_H}$ manually.

Anal. UV-vis (λ, nm): 357; 414; 488; 554; 608; 715. ESI-MS (CH_2Cl_2): 2363.16 ($[Au_{20}(Ph_3P)_{12}H_3]^{3+}$) and 2364.14 ($[Au_{20}(Ph_3P)_{12}D_3]^{3+}$) and ^2H NMR (500MHz, $CHCl_3$, δ, ppm): 4.69. ^{31}P NMR (202 MHz, CD_2Cl_2, δ, ppm): 56.56.

$[Au_{20}(PPh_3)_{12}H_2$(2-COOH-PhS)$](PF_6)_3$ (2_H)

To a solution of Ph_3PAuCl (49 mg, 0.10 mmol) in CH_2Cl_2 (2.0 mL), 2-COOH-PhSH (15 mg, 0.10 mmol) and HPF_6 (60 wt.% in water, 25 μL, 0.10 mmol) were added. Then a freshly prepared solution of $NaBH_4$ (3.8 mg in 1.0 mL of ethanol) was added dropwise with vigorous stirring. The ratio of $Ph_3PAuCl/NaBH_4$ is about 1:1. The solution color changed from colorless to pale brown and finally to dark brown. After stirring overnight at room temperature in the dark, the reaction was evaporated to dryness to give a dark brown solid. The solid was washed with ether (2×5.0 mL), then dissolved in 2.5 mL CH_2Cl_2, and the resulted solution was centrifuged for 3 min at 10000 r.min^{-1}. The brown supernatant was collected and subjected to vapor diffusion with n-pentane to afford brown crystals after 7 days in 5% yield.

Anal. UV-vis (λ, nm): 339; 386; 424; 467; 603; 700. ESI-MS (CH_2Cl_2): 2413.82 ($[Au_{20}(PPh_3)_{12}H_2$(2-COOH-PhS)$]^{3+}$) and 2414.67 ($[Au_{20}(PPh_3)_{12}D_2$(2-COOH-PhS)$]^{3+}$). ^2H NMR (500 MHz, $CHCl_3$, δ, ppm): 2.39.

Following the aforementioned procedures, the deuteride clusters $[Au_{20}(PPh_3)_{12}D_3](SbF_6)_3$ (**1D)** and $[Au_{20}(PPh_3)_{12}D_2(2\text{-}COOH\text{-}PhS)](PF_6)_3$ (**2D)** can also be obtained by using $NaBD_4$ instead of $NaBH_4$.

III. Computational details

Density functional theory (DFT) calculations were performed with the quantum chemistry program Turbomole V6.4 and Gaussian 16.[1-2] The Ph groups in cluster **1H** was replaced by CH_3 in order to save computation time in the calculations. Starting from the structure date of the observed single crystal X-ray crystallography of $[Au_{20}(PPh_3)_{12}H_3]^{3+}$, we carried out full geometry optimization of the model cluster $[Au_{20}(PMe_3)_{12}H_3]^{3+}$.

In Turbomole calculations, geometry optimization and Time-dependent DFT calculation of the UV-vis absorption spectra were done with the functional of Perdew, Burke and Ernzerhof (PBE).[3-6] The def2-TZVP basis sets were used for all of the C, H, N, P and Au atoms.[7] The calculations were performed without symmetry constraints, and the resolution of the identity method was used to speed up calculations. The TD-DFT calculations evaluate lowest 50 singlet-to-singlet excitation energies.

In Gaussian calculations, geometry optimization was done with the functional of B3LYP, and the 6-31G(d) basis set is used for C, P and H, and LANL2DZ for Au.[2,8] The ^1H NMR calculations were computed using the gauge-including atomic orbital (GIAO) approach at the following levels of theory: PBE0/Def2-TZVP, PBE0/genecp (pcSseg-1 basis sets were used for C, P, H, and LANL2DZ for Au), B972/Def2-TZVP, B972/genecp (pcSseg-1 basis sets were used for C, P, H, and LANL2DZ for Au), B3LYP/Def2-TZVP and B3LYP/ genecp (pcSseg-1 basis sets were used for C, P, H, and LANL2DZ for Au), respectively.[9-11] The parameters of pcSseg-1 basis set were obtained from the well-known basis set exchange portal.[12] Total chemical shifts of atoms were defined as $\sigma = \sigma_{TMS} - \sigma_{cluster}$, where σ_{TMS} and $\sigma_{cluster}$ are, respectively, the isotropic chemical shielding of ^1H in tetramethylsilane and in the $[Au_{20}(PMe_3)_{12}H_3]^{3+}$ cluster.

References:

(1) F. Furche, and R. Ahlrichs, *J. Chem. Phys.*, **2002**, *117*, 7433-7447.

(2) M. J. Frisch, G. W. Trucks, H. B. Schlegel, G. E. Scuseria, M. A. Robb, J. R. Cheeseman, G. Scalmani, V. Barone, B., Mennucci, G. A. Petersson, H. Nakatsuji, M. Caricato, X. Li, H. P. Hratchian, A. F. Izmaylov, J. Bloino, G. Zheng, J. L. Sonnenberg, M. Hada, M. Ehara, K. Toyota, R. Fukuda, J. Hasegawa, M. Ishida, T. Nakajima, Y. Honda, O. Kitao, H. Nakai, T. Vreven, J. A. Montgomery, J. E. Jr. Peralta, F. Ogliaro, M. Bearpark, J. J. Heyd, E. Brothers, K. N. Kudin, V. N. Staroverov, R. Kobayashi, J. Normand, K. Raghavachari, A. Rendell, J. C. Burant, S. S. Iyengar, J. Tomasi, M. Cossi, N. Rega, J. M. Millam, M. Klene, J. E. Knox, J. B. Cross, V. Bakken, C. Adamo, J. Jaramillo, R. Gomperts, R. E. Stratmann, O. Yazyev, A. J. Austin, R. Cammi, C. Pomelli, J. W. Ochterski, R. L. Martin, K. Morokuma, V. G. Zakrzewski, G. A. Voth, P. Salvador, J. J. Dannenberg, S. Dapprich, A. D. Daniels, O. Farkas, J. B. Foresman, J. V. Ortiz, J. Cioslowski, D. J. Fox, Gaussian 16, revision C.01, Gaussian, Inc.: Wallingford, CT, 2016.

(3) Becke, A. D. *Phys. Rev. A*, **1988**, *38*, 3098-3100.

(4) J. P. Perdew, *Phys. Rev. B*, **1986**, *33*, 8822-8824.

(5) J. P. Perdew, K. Burke, and M. Ernzerhof, *Phys. Rev. Lett.*, **1996**, *77*, 3865-3868.

(6) R. Ahlrichs, M. Bär, M. Häser, H. Horn, and C. Kölmel, *Chem. Phys. Lett.*, **1989**, *162*, 165-169.
(7) F. Weigend, R. Ahlrichs, *Phys. Chem. Chem. Phys.*, **2005**, *7*, 3297-305.
(8) P. J. Hay, W. R. J. Wadt, *Chem. Phys.*, **1985**, *82*, 299-310.
(9) K. Wolinski, J. F. Hinton, P. Pulay, *J. Am. Chem. Soc.,* **1990**, *112*, 8251-8260.
(10) R. P. Silalahi, G. Huang, J. Liao, T. Chiu, K. K. Chakrahari, X. Wang, C. W. Liu, *Inorg. Chem.,* **2020**, *59*, 2536-2547.
(11) F. Jensen, *J. Chem. Theory Comput.*, **2015**, *11*, 132-138.
(12) B. P. Pritchard, D. Altarawy, B. Didier, T. D. Windus, T. L. Gibson, *J. Chem. Inf. Model.*, **2019**, *59*, 4814-4820.
(13) B. Delley, *J. Chem. Phys.,* 1990, **92**, 508-517; *J. Chem. Phys.,* 2003, **113**, 7756-7764. Dmol3 is available from Accelrys.

IV. Supporting figures

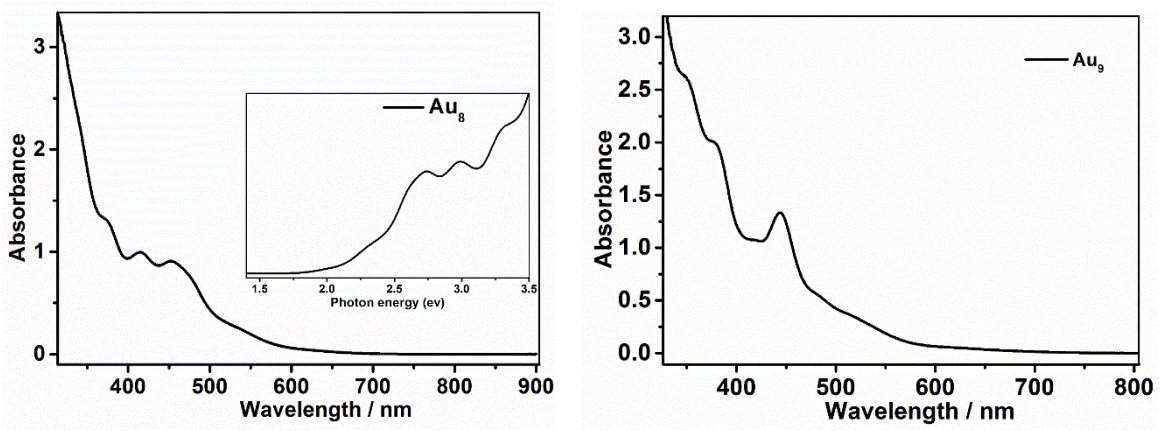

Figure S1. The identification of the by-products (Au_8 and Au_9) in the synthesis of $[Au_{20}(PPh_3)_{12}H_3](SbF_6)_3$ by optical spectra. ($Au_8 = [Au_8(PPh_3)_8]^{2+}$ and $Au_9 = [Au_9(PPh_3)_8]^{3+}$)

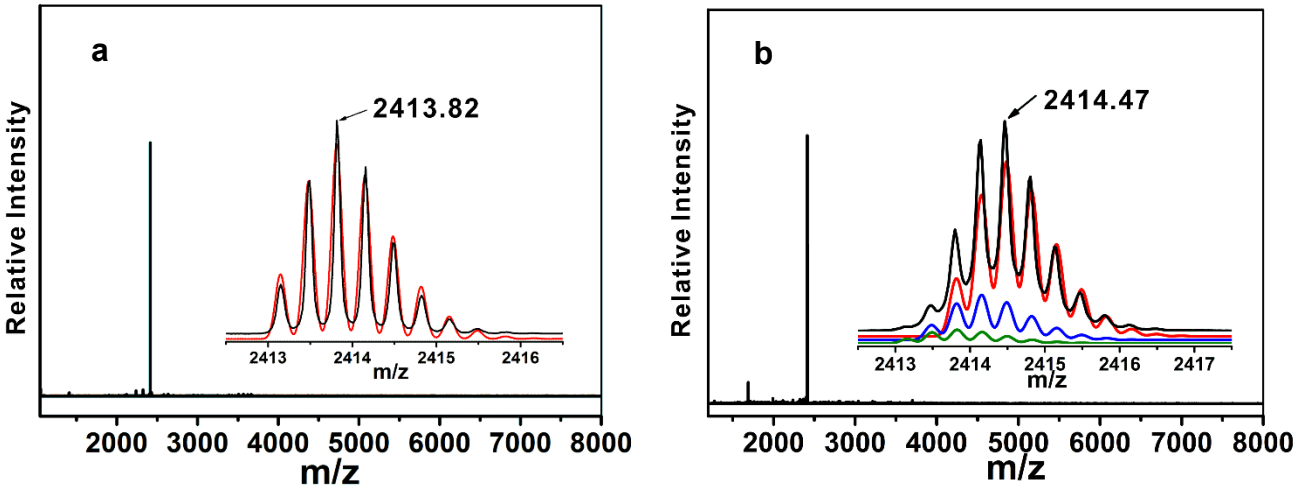

Figure S2. Mass spectra of $[Au_{20}(PPh_3)_{12}H_2(2\text{-COOH-PhS})](PF_6)_3$ and the deuteride analogue. Inset: (a) the experimental (black trace) and simulated (red trace) isotopic patterns of molecular ion peak $[Au_{20}(PPh_3)_{12}H_2(2\text{-COOH-PhS})]^{3+}$ and (b) the experimental (black trace) and simulated (red trace) isotopic patterns of molecular ion peak $[Au_{20}(PPh_3)_{12}D_2(2\text{-COOH-PhS})]^{3+}$, simulated (blue trace) isotopic patterns of $[Au_{20}(PPh_3)_{12}DH(2\text{-COOH-PhS})]^{3+}$ and simulated (green trace) isotopic patterns of $[Au_{20}(PPh_3)_{12}H_2(2\text{-COOH-PhS})]^{3+}$.

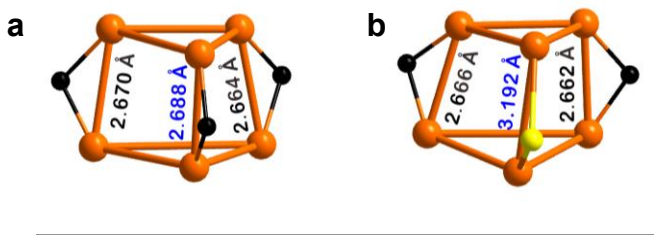

Figure S3. (a) $[Au_6H_3]$ motif in cluster $\mathbf{1_H}$ and (b) $[Au_6H_2S]$ motif in cluster $\mathbf{2_H}$. Show both of the three interface bond Lengths. Atom colors: orange = Au, black = H, purple = P, yellow = S, gray = C; the positions of hydrides are hypothetic.

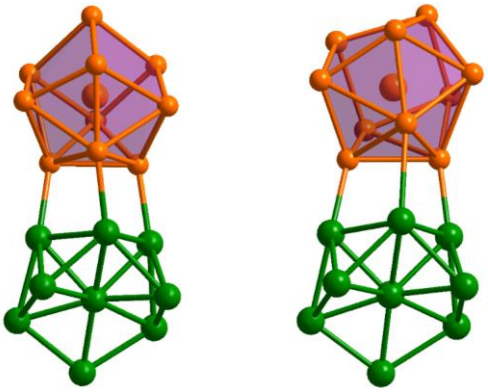

Figure S4. Comparison of the Au_{20} core structures of cluster $\mathbf{1_H}$ (left) and $\mathbf{2_H}$ (right).

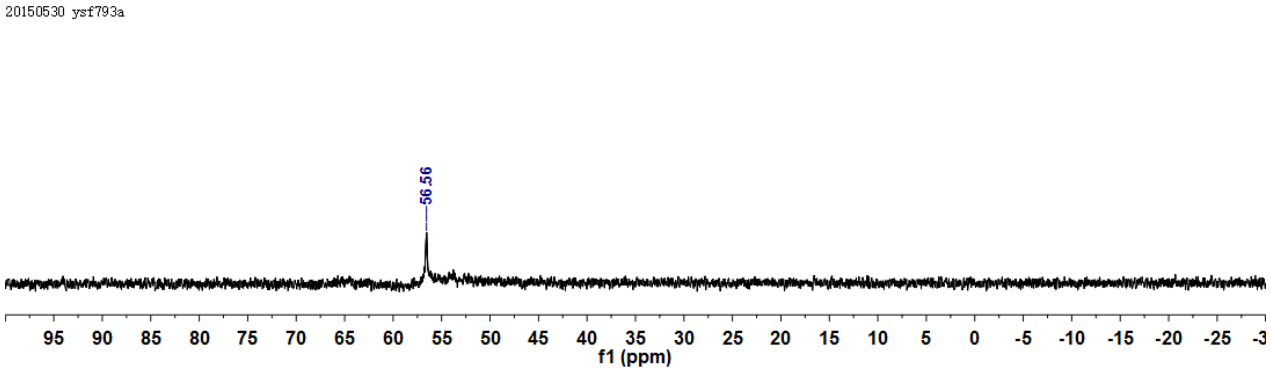

Figure S5. ^{31}P NMR spectroscopy of $[Au_{20}(PPh_3)_{12}H_3](SbF_6)_3$ in CD_2Cl_2.

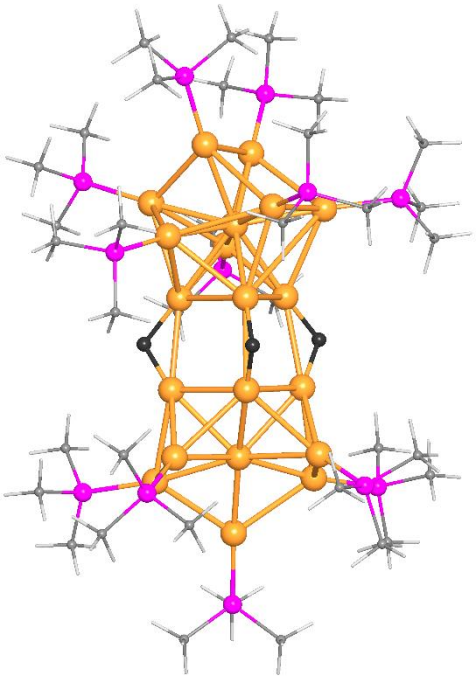

Figure S6. Optimized structure of $[Au_{20}(PPh_3)_{12}H_3]^{3+}$ cluster. CH_3 group was used as a substitute of Ph in the Ph_3P ligand for simplification. Atom colors: orange= Au; purple= P; gray= C; white= H. Three hydrides were highlighted in black balls.

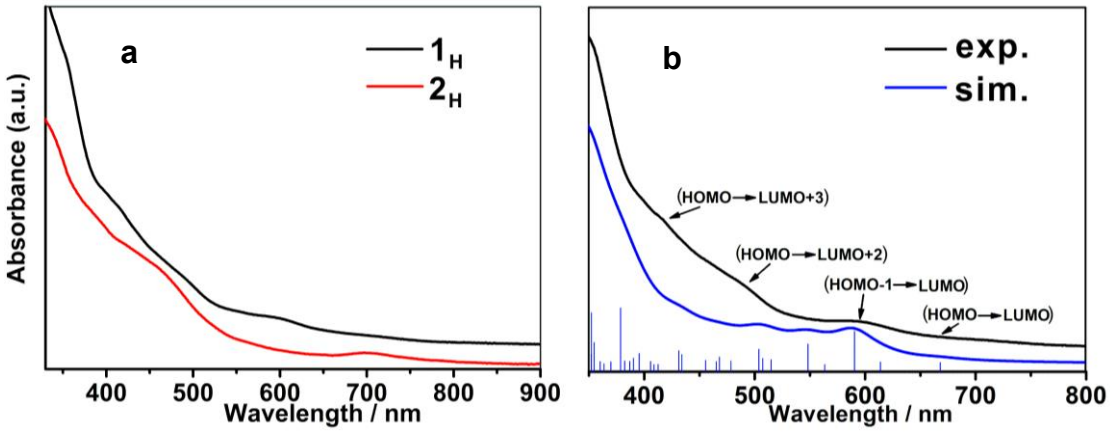

Figure S7. (a) Comparison of optical spectra of $\mathbf{1_H}$ and $\mathbf{2_H}$ in CH_2Cl_2. (b) Experimental and calculated UV-vis spectra of $\mathbf{1_H}$.

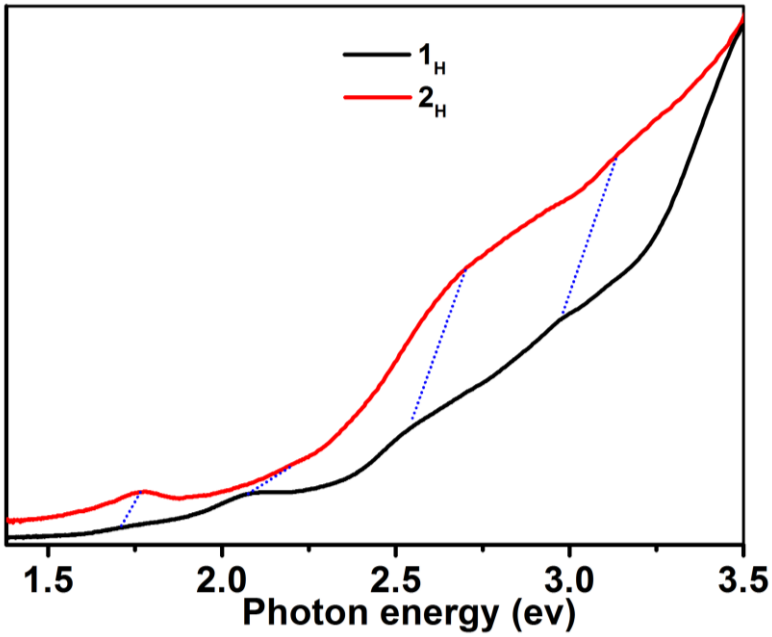

Figure S8. Comparison of optical spectra of **1H** and **2H** at eV energy scale.

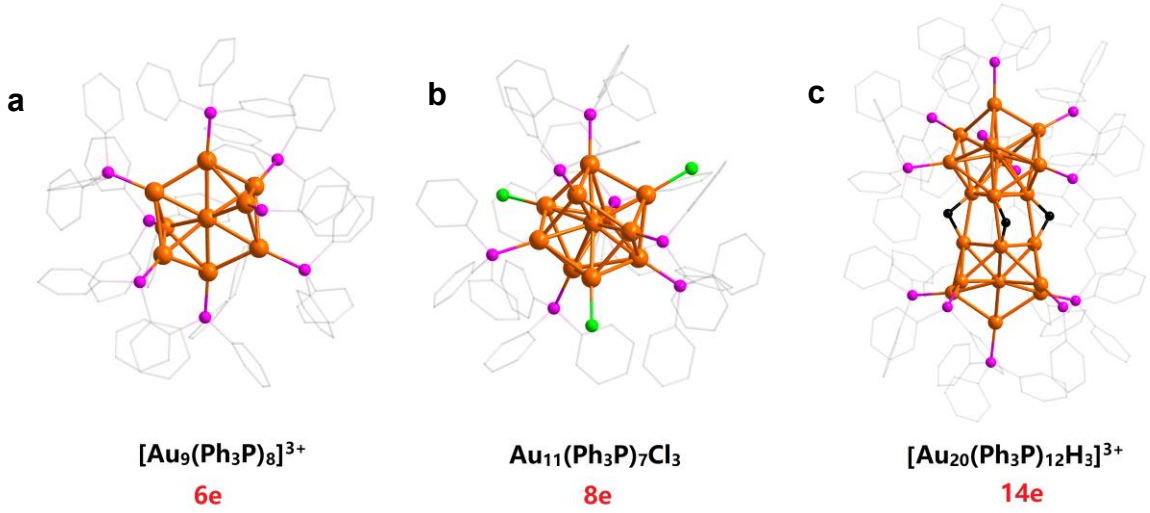

Figure S9. Structural comparison of (a) $[Au_9(Ph_3P)_8]^{3+}$, (b) $Au_{11}(Ph_3P)_7Cl_3$, (c) $[Au_{20}(Ph_3P)_{12}H_3]^{3+}$.

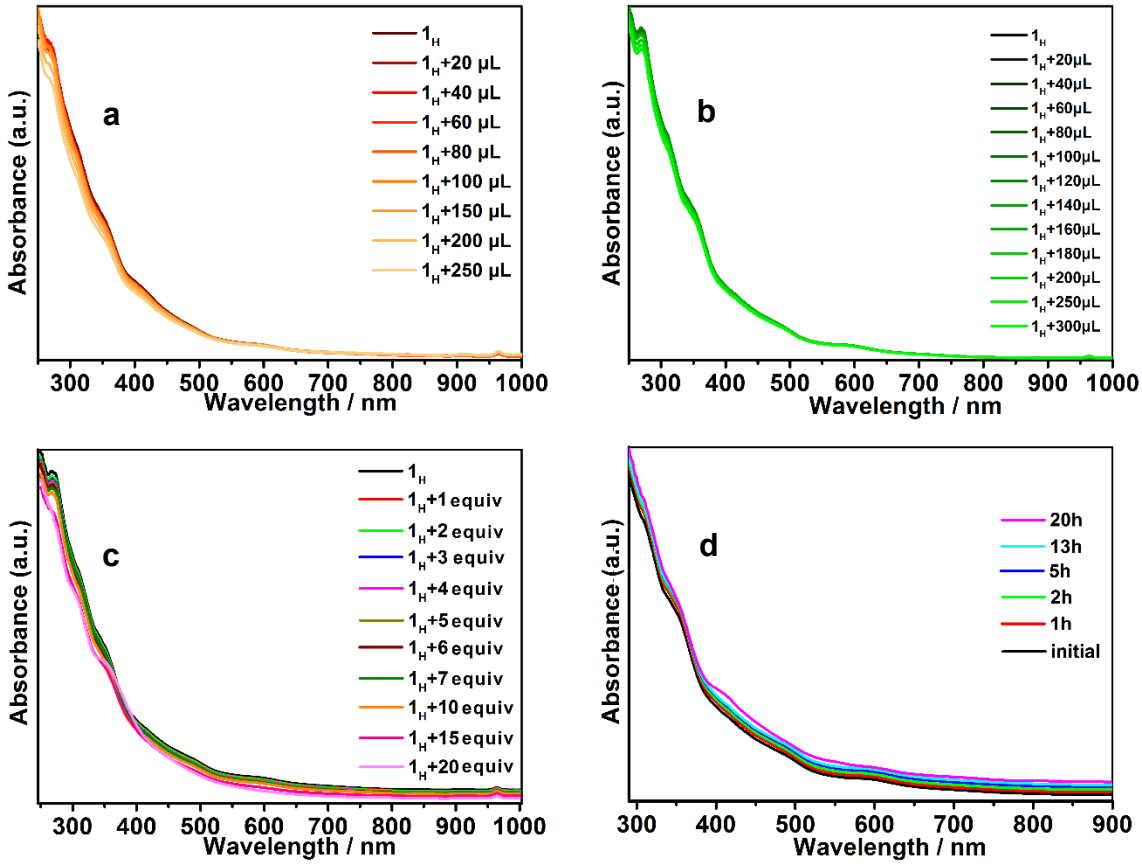

Figure S10. Time-dependent UV-Vis spectra of **1H** for monitoring stability under various conditions. (a) acidic environment: 2 mL 2.5 μM Au_{20} in CH_2Cl_2 and mixed with different portions of 0.1 M HPF_6 in MeOH; (b) alkaline environment: 2 mL 2.5 μM Au_{20} in CH_2Cl_2 and mixed with different portions of 0.1 M MeONa in MeOH; (c) 2-COOH-PhSH added experiment: 2 mL 2.5 μM Au_{20} in CH_2Cl_2 and added different equivalents of 2-COOH-PhSH in MeOH; (d) high temperature environment: Au_{20} (2 mg) was dissolved in 1 mL CH_2Cl_2 and 3 mL toluene at 70 °C.

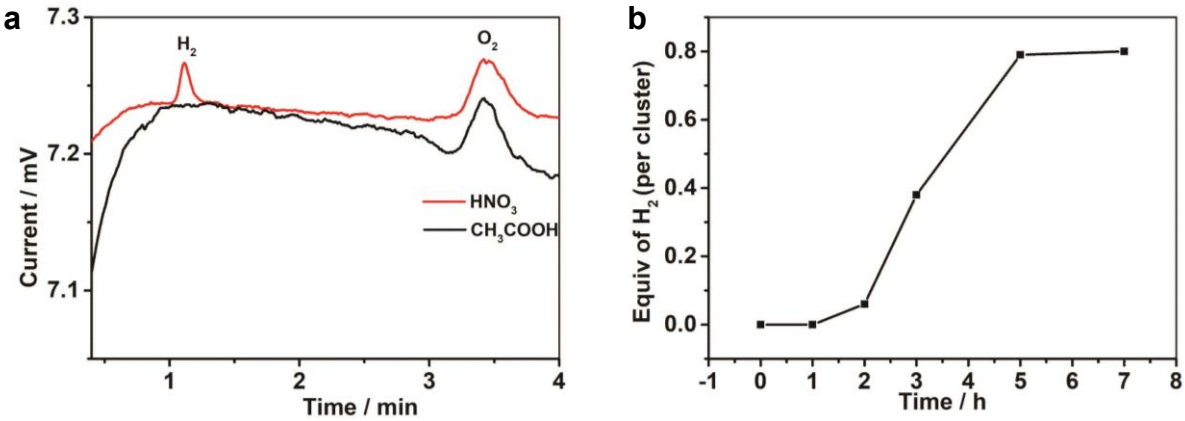

Figure S11. GC Analysis：(a) Conditions: 2 mg **1H** was dissolved in 10 mL DMF and in the presence of 1 mL CH_3COOH (black) or HNO_3 (red) for 1 h. (b) Conditions: 2 mg **1H** was dissolved in 10 mL DMF and heated at 100 °C for various times.

Table S1. Selected structural parameters and the corresponding DFT computed values.

	Bond length (Å)		
	bond	**X-ray**	**DFT**
Cluster 1	**Au-H**	**---**	**1.744-1.798**
	Au-Au within Au_{11}	**2.6329(8)−3.1475(8)**	**2.701-3.216**
	Au-Au within Au_9	**2.6395(8)–2.9559(8)**	**2.700-2.959**
	Au-Au (H)	**2.6641(8)-2.6698(8)**	**2.743-2.752**
	Au-P	**2.276(4)-2.306(4)**	**2.325-2.356**
Cluster 2	**Au-H**	**---**	**---**
	Au-S	**2.383(3)-2.388(3)**	**---**
	Au-Au (H)	**2.6614(6)-2.6659(6)**	**---**
	Au-Au (S)	**3.1920(7)**	**---**

Table S2. The ^{2}H NMR results of $\mathbf{1_D}$ and the corresponding DFT computed values. NMR shifts (minimum and maximum) are shown in brackets.

Atoms	**NMR shifts (ppm)**						
	Expt. (^{2}H)	**Calc. (^{1}H)**					
Hydrides	**4.69**	**b3lyp-pcSseg**	**b972-pcSseg**	**pbe0-pcSseg**	**b3lyp-tzvp**	**b972-tzvp**	**pbe0-tzvp**
		5.57 (5.00-6.48)	**5.73 (5.17-6.66)**	**5.67 (5.06-6.59)**	**5.33 (4.69-6.40)**	**5.62 (4.99-6.72)**	**5.57 (4.93-6.66)**
CH_3-(H)	**---**	**1.75 (1.46-2.31)**	**1.78 (1.49-2.33)**	**1.87 (1.55-2.38)**	**1.49 (1.24-2.99)**	**1.53 (1.29-2.05)**	**1.65 (1.39-2.15)**

Table S3. The Mulliken, natural bond orbital (NBO), and Hirshfeld charge distribution for $[Au_{20}H_3P(CH_3)_3)_{12}]^{3+}$. Charge variations (minimum and maximum) are shown in brackets. The Mulliken and NBO charge distributions are obtained from Gaussian 09, and Hirshfeld charge distribution is obtained from Dmol3.[13]

	Num.	Mulliken	NBO	Hirshfeld
Charge/Au in Au_{11} inner core	1	3.872	-2.161	-0.0448
Charge/Au in Au_9 inner core	1	0.419	-1.032	-0.0530
Charge/Au in Au-$[P(CH_3)_3]$ of Au_{11}	7	-0.871 (-0.996, -0.729)	0.184 (0.160, 0.229)	-0.0312 (-0.0424, -0.0194)
Charge/Au in Au-$[P(CH_3)_3]$ of Au_9	5	-0.733 (-0.992, -0.549)	0.138 (0.102, 0.161)	-0.0241 (-0.0534, -0.0107)
Charge/$P(CH_3)_3$ in Au-$[P(CH_3)_3]$	12	0.702 (0.661, 0.722)	0.991 (0.982, 1.005)	0.2691 (0.2642, 0.2762)
Charge/Au in Au_6 interface	6	0.022 (-0.662, 0.578)	0.077 (-0.011, 0.113)	-0.0286 (-0.0327, -0.0249)
Charge/H bridging in Au_6 interface	3	0.080 (0.071, 0.098)	-0.203 (-0.210,-0.197)	-0.0991 (-0.1066, -0.0951)